Influence of Anesthetic and Nonimmobilizer Molecules on the Physical Properties of a Polyunsaturated Lipid Bilayer

Laure Koubi,[†] Leonor Saiz,*[,†,‡] Mounir Tarek,[†,‡,§] Daphna Scharf,[†,||] and Michael L. Klein[†]

Center for Molecular Modeling and Chemistry Department, University of Pennsylvania, 231 South 34th Street, Philadelphia, Pennsylvania 19104-6323, NIST Center for Neutron Research, Materials Science and Engineering Laboratory, National Institute of Standards and Technology, 100 Bureau Drive, Stop 8562, Gaithersburg, Maryland 20899-8562, Equipe de Dynamique des Assemblages Membranaires, Unité Mixte de Recherche C.N.R.S./U.H.P. No. 7565, Universite Henri Poincaré—Nancy I, B.P. 239, F-54506 Vandoeuvre-lès-Nancy Cedex, France, Department of Anesthesia, Medical Center, University of Pennsylvania, 3620 Hamilton Walk, Philadelphia, Pennsylvania 19104-4283

Received: April 30, 2003; In Final Form: September 23, 2003

We use molecular dynamics simulations to investigate the effects of halothane, a volatile anesthetic, and hexafluoroethane (HFE), its nonimmobilizer analogue, on the physical properties of a fully hydrated polyunsaturated (1-stearoyl- 2-docosahexaenoyl-*sn*-glycero-3-phosphocholine) lipid bilayer in the liquid crystalline fluid lamellar phase, L_α. In addition, we discuss the results obtained comparing them to previous studies on saturated lipid bilayers with the same solutes. At the analyzed concentration (25% mole fraction), the halothane molecules are located preferentially near the upper part of the lipid acyl chains, while the HFE molecules prefer the hydrocarbon chains and methyl trough region. In the case of halothane in the polyunsaturated lipid bilayer, there is an additional density maximum at the membrane center not observed in saturated lipids. The subtle effect of the solutes on the structural properties of the highly unsaturated lipid bilayer and the properties of the membrane interior is somewhat different from that observed for saturated lipids. Here, these differences are interpreted in terms of the unique properties of the polyunsaturated lipid bilayers. The effect of anesthetic molecules on the electrostatic properties of the membrane interface is similar for saturated and polyunsaturated lipid bilayers and is characterized by a change in the most probable orientation of the lipid headgroup dipoles, which point toward the membrane interior for halothane and are basically unchanged for HFE, i.e., point toward the water phase. The different distributions of anesthetic and nonimmobilizer molecules within the lipid bilayer systems seem to be a generic feature in simple models of biological membranes and are similar to those observed in systems with saturated lipids. Since polyunsaturated and other unsaturated lipids are ubiquitous in cell membranes, it is plausible to generalize these features to the more complex biological membranes.

I. Introduction

Deciphering the molecular mechanism of action of inhaled anesthetics (IAs) remains a challenge despite 150 years of clinical usage.[1] The site of anesthetic action is indeed uncertain, and very little definitive information exits on the molecular level action of IAs. The controversy as to whether the IAs primary site of action is the lipid membrane or the membrane proteins is still a matter of debate. The high solubility of IAs in lipids suggests that the anesthetics may act on the lipid bilayer, where membrane proteins are embedded. This is supported by experimental evidence of modification of membrane structure and/or phase state at sufficiently high anesthetic concentrations.[2−5] In contrast, several studies suggest that the association of IAs with cellular proteins (ion channels)[6−8] alter their activity. The nature of the molecular interactions leading to protein function modification remains still unclear. Recently, a renewed interest in the role of membrane lipids was ignited by a hypothesis from Cantor. He suggested that modifications in membrane structure induced by the presence of IAs may indirectly alter membrane protein function.[9−11]

The correlation of IA potency with their solubility in oil, generally known as the Meyer−Overton rule,[12] has served for many years to predict anesthetic potency.[6,13] Recently, a number of compounds with structures and oil solubilities similar to those of known IAs and, therefore, predicted to be good anesthetics by the Meyer−Overton rule were found to lack anesthetic properties.[14−16] These molecules, known as nonimmobilizers (also called nonanesthetics), do not suppress movement but cause amnesia. Consequently, it has been suggested that different mechanisms may be responsible for anesthesia and immobility.[17−20] This has triggered an interest in comparative studies of the effects of nonimmobilizers and anesthetics to better understand the mechanisms of IA action. Several experimental studies were aimed at identifying the nature of the interactions between anesthetic molecules and simple lipid bilayer membranes. In general, the anesthetics seem to reside preferentially in the lipid hydrocarbon chain domain, near the lipid headgroup.[21−24] NMR experiments have revealed that the orientational order of the lipid chains is slightly higher near the headgroups and is lower near the chain ends than that of

* Author to whom correspondence may be addressed. E-mail: leonor@cmm.chem.upenn.edu.
[†] Chemistry Department, University of Pennsylvania.
[‡] National Institute of Standards and Technology.
[§] Université Henri Poincaré—Nancy I.
[||] Department of Anesthesia, Medical Center, University of Pennsylvania.

10.1021/jp035169o CCC: $25.00
Published on Web 12/02/2003

the pure lipid bilayers.[25,26] Similar studies on nonimmobilizer molecules have shown differences from their anesthetic counterparts. The results indicated that the addition of nonimmobilizers in lipid membranes induces little or no modification of the orientational order of the chains.[26]

Computer simulations provide a unique tool to analyze biomembrane properties from an atomic perspective with a level of detail missing in any other technique.[27,28] Classical molecular dynamics (MD) studies on anesthetics and nonimmobilizers incorporated in simple model membranes were recently conducted to obtain a molecular-level picture of the interactions and effects of these two types of solutes on lipid bilayers. The computation of the free-energy profiles of the solutes in a simple lipid bilayer by Pohorille and co-workers[29−31] showed that nonimmobilizers are driven from the interface into the membrane interior, while anesthetics are not. Our previous MD simulation studies of the anesthetic halothane incorporated within saturated lipid bilayers[32,33] indicated that the molecules are indeed located in the upper part of the lipid acyl chains, in contact with the lipid−water interface. Our results showed that the halothane modified the structure of the membrane without exhibiting specific interactions with the lipids at clinical concentrations.[32] Several structural modifications of the lipid bilayer when halothane was added were identified. These included a lateral expansion of the lipid membrane, a decrease of the alkyl chains orientational order parameters for the tail end region, and a modification of the orientation of the headgroup dipole. In contrast, hexafluoroethane (HFE), a halothane nonimmobilizer analogue, was found to induce almost no changes in the structure of the lipid bilayer.[34,35] These differences seem to be related to their homogeneous distribution along the lipid hydrocarbon chains.

Previous MD simulations of simple membrane models focused mainly on the study of saturated lipids.[28] The excellent agreement obtained with experiment demonstrated the ability of the current force fields and simulation methodologies to reproduce reasonably well the structural and dynamical properties of membranes with saturated lipids or lipids with a low degree of unsaturation. Many important biological membranes, such as those found in the retina or the brain tissue, contain, however, a considerable amount of phospholipid molecules with highly unsaturated (containing double bonds) acyl chains.[36] The presence of cis double bonds in lipid bilayers is known to affect a number of physical properties of membranes, such as enhanced permeability to small molecules,[37,38] enhanced elasticity or decrease in the area compressibility modulus,[39,40] and low main order−disorder phase-transition temperatures.[41,42] Very recent computer simulation studies[43−47] of 1-stearoyl-2-docosahexaenoyl-*sn*-glycero-3-phosphocholine (SDPC, 18:0/22:6ω3 PC) lipid bilayers in the fluid lamellar phase, L_α, have improved our understanding of the microscopic origin of the effect of cis double bonds on the properties of lipid bilayers.

In the present study, which to the best of our knowledge constitutes the first computational attempt to investigate the mechanisms of anesthesia action in highly unsaturated membranes, we extend our previous computer simulations on anesthetic and nonimmobilizer molecules embedded in lipid bilayers to investigate how these solutes affect the properties of lipid bilayers with polyunsaturated acyl chains. Here, we present the results obtained in two MD simulations of fully hydrated SDPC lipid bilayers, containing each 25 mol % of the anesthetic halothane or of the nonimmobilizer HFE. In addition, we compare the findings to our previous investigations of both molecules in dipalmitoylphosphatidylcholine (DPPC) and dimyristoylphosphatidylcholine (DMPC) lipid bilayers[32−35] and to the results of a pure SDPC bilayer at similar conditions.[43−45,48]

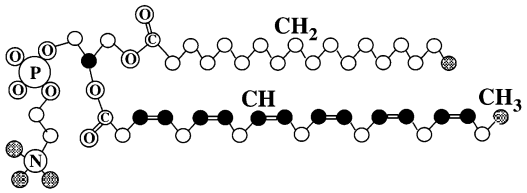

Figure 1. Schematic representation of the SDPC lipid molecules. The CH, CH_2, and CH_3 groups are displayed in black, white, and gray (pattern), respectively, and the remaining atoms (P, N, O, C) are labeled individually. The hydrogen atoms, all considered explicitly in the simulations as interaction sites, are omitted for clarity. The single and double covalent bonds of the two fatty acid units are shown as single and double lines, respectively.

II. Methods

The SDPC lipid molecules are composed of two acyl chains and a neutral phosphatidylcholine (PC) headgroup. The saturated stearoyl acid is located at the sn1 position, while the highly unsaturated docosahexaenoic acid (DHA) is located at the sn2 position. The saturated and polyunsaturated chains contain 18 and 22 carbon atoms, respectively. In addition, the DHA chain is characterized by six cis double bonds. For the sake of clarity, we show a cartoon of an SDPC lipid molecule in Figure 1.

To study the effect of anesthetic (halothane) and nonimmobilizer (HFE) molecules on the properties of lipid bilayers with highly unsaturated acyl chains at conditions relevant to biology, we performed MD simulations on fully hydrated model membranes in the fluid lamellar phase. Thus, the temperature of the systems was set to $T = 30$ °C, which lays well above the gel to liquid crystalline phase transition temperature (approximately −6.5 °C).[41] The initial configuration for the simulations was taken from a well-equilibrated fully hydrated SDPC lipid bilayer.[43] The pure SDPC lipid bilayer consisted of 64 lipid molecules (32 per leaflet) and 27.5 water molecules per lipid and was characterized by a surface area per lipid molecule of $A = 61.4$ Å^2 (1 Å $= 10^{-10}$ m) and a lamellar spacing (repeated distance) of $d = 70.0$ Å.[43] For each of the two studied systems (SDPC/halothane and SDPC/HFE), 16 molecules of either halothane or HFE, which corresponds to a mole fraction of 25%, were uniformly incorporated in the lipid bilayer hydrophobic region. This initial configuration of the solutes is consistent with the large lipid−water partition coefficient for halothane and other halogenated compounds.[14,49] Following the process described previously,[32] the solute molecules were initially treated as point masses with zero charges and zero van der Waals parameters in order to avoid strongly repulsive interactions with the lipid molecules. By use of short consecutive MD simulation runs, the solute molecules were grown stepwise by extending their intramolecular bonds and augmenting their interactions with the surrounding medium. After a 200-ps initial equilibration run for each system at constant number of particles, constant volume, and constant temperature (NVT ensemble), the MD simulations were continued for an additional 3.7 ns at constant pressure, $p = 1$ atm (1 atm = 101.3 kPa), and constant temperature, $T = 30$ °C (NPT ensemble). Unless otherwise stated, the different properties were evaluated over the last 1 ns of the two NPT runs, where the distribution of solute molecules reaches its equilibrium.

The MD simulation studies described herein were carried out using the recently developed molecular dynamics package (PINY_MD).[50] The NPT runs were performed using the Nosé−

Hoover chain thermostat extended system method[51] with separate thermostats for the lipid, water, and HFE or halothane molecules and using an orthorhombic simulation cell and the usual periodic boundary conditions. A reversible multiple time step algorithm was used to integrate the equations of motion with the largest (smallest) time step of 5 fs (1 fs). The electrostatic interactions were calculated using the Particle−Mesh−Ewald (PME) method.[52,53] The minimum image convention[54] was employed to calculate the Lennard-Jones interactions and the real-space part of the Ewald sum using a spherical truncation for the short- and long-range parts of the force decomposition of 7 and 10 Å, respectively. SHAKE/ROLL and RATTLE/ROLL methods were used to constrain all bonds involving hydrogen atoms to their equilibrium values.[51]

The molecular and potential model used for the lipid molecules was the all-atom CHARMM force field and parameters[55,56] and the TIP3P model for water.[57] Previous simulations have shown that this force field reproduces rather well the structure of bilayers composed of phospholipids with cis double bonds.[43,46,47,58,59] As discussed in ref 43, the model used underestimates the area per lipid of the pure lipid bilayer (by 10%). It captures, however, the important features of SDPC lipids and reproduces qualitatively and semiquantitatively the experimental data (for more details, see refs 43−45). Very recently and after this study was performed, a specific CHARMM force field has been developed for this particular lipid and closer agreement with experiment has been achieved,[46] confirming the results obtained earlier by Saiz and Klein. That recent simulation, however, was performed at a fixed area within the plane of the membrane interface, and thus, it has not been shown yet if this new model reproduces better the experimental area per lipid of the system without using it as a constraint. Ideally, one would like to use the same force field for all the components of the system under study. In the case of halothane and HFE, however, to the best of our knowledge, there is no CHARMM parametrization available. Thus, for the halothane molecules ($CF_3CHClBr$), we employed the parameters developed by Scharf and Laasonen[60] and used in our previous studies of the DPPC/halothane system.[32,33] The set of parameters used for the HFE (C_2F_6) molecules were taken from ref 35. The parameters were fitted following the same methodology used in our previous work on halothane.[60] The same parameters were used in our previous DMPC/HFE study.[34,35]

III. Results and Discussion

A. Membrane Structure. The time evolution of the calculated area per lipid (A) and the lamellar spacing (d) of the SDPC lipid bilayer are displayed in Figure 2. The initial structure at $t = 0$ ps corresponds to that of the pure SDPC lipid bilayer characterized by a lamellar spacing $d \simeq 70.0$ Å and an area per lipid $A \simeq 61.4$ Å^2.[43] Figure 2 shows that the system undergoes only small fluctuations for the first 1.5 ns. Toward the end of the simulation, the average surface area per lipid and the lamellar spacing fluctuate around $A = 58$ Å^2 and $d = 75$ Å, respectively, for both halothane/SDPC and HFE/SDPC systems with standard deviations of about 1.5 Å^2 and 1.0 Å, respectively, which are similar to those observed in other simulation studies of lipid bilayers in the fluid lamellar phase.

The effect of including halothane and HFE molecules in the pure SDPC lipid bilayer consists of an increase of the interlamellar spacing of about 7% and a decrease of the area per molecule of 5%.

B. Distribution of the Solute Molecules in the Membrane. The most relevant observation of previous studies of anesthetic and nonimmobilizer molecules in lipid bilayers is the nonuniform distribution of anesthetics along the direction perpendicular to the membrane surface or membrane normal. While anesthetics and nonanesthetics have similar solubilities in olive oil, their distributions within the model membrane differ. To illustrate the differences obtained for halothane and HFE molecules, we show the instantaneous configurations of the SDPC/halothane and the SDPC/HFE systems extracted from the MD simulations at different times in Figure 3. In Figure 3a, which corresponds to the instantaneous configurations at the end of the initial 200 ps of the NVT equilibration run, the anesthetic and the nonimmobilizer molecules are still evenly distributed within the lipid bilayer. After 2.2 ns, a new distribution pattern develops (Figure 3b). The halothane molecules seem to be preferentially located in the upper part of the SDPC lipid acyl chains and at the bilayer center (methyl trough). Conversely, the nonimmobilizer molecules prefer the center of bilayer hydrophobic core. These trends are clearly emphasized in Figure 3c, which corresponds to the end of the simulations (3.9 ns).

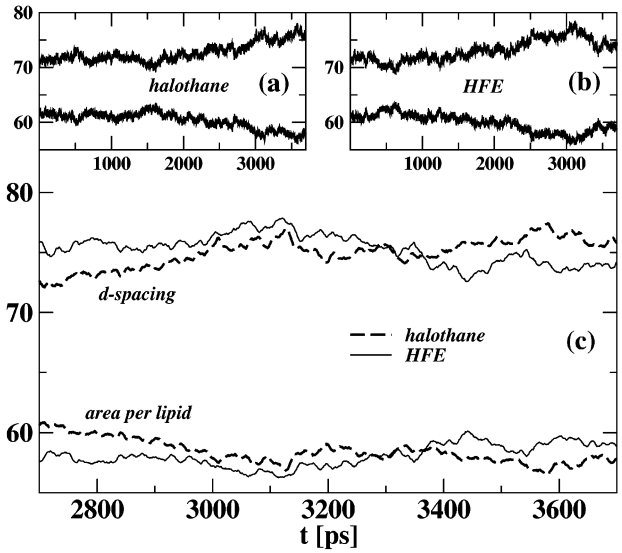

Figure 2. Time evolution of the area per lipid, A, in Å^2 and the lamellar spacing, d (denoted d spacing), in Å during the 3.7 ns of the NPT MD simulations. (a) SDPC/halothane system, (b) SDPC/HFE system, and (c) both systems for the last 1 ns.

To quantitatively evaluate the distributions of the solutes within the lipid bilayer, we calculated the average electron density distributions of the different components along the bilayer normal, Z, or electron-density profiles. The curves corresponding to the halothane and HFE molecules are reported in Figure 4 together with the density profiles of the lipid and water molecules and the phosphate group of the lipid headgroups to highlight the position of the lipid−water interface. The density profile of anesthetic molecules shows a bimodal component, indicating an increase of number of halothane molecules near the upper part of the acyl chains (10 Å $< |Z| <$ 18 Å), which is in close contact with the water region. We have also observed another maximum at the bilayer center due to a concentration increase at the methyl trough (0 Å $< |Z| <$ 5 Å). For the HFE molecules, the distribution is quite different. The nonimmobilizer molecules seem to be located mostly at the bilayer center (0 Å $< |Z| <$ 9 Å), without any affinity with the upper part of the acyl chains or the interface. Further analysis indicates that the maxima of the halothane density profiles at the interface are located around the carbon atom C5 of the saturated chain and the carbon atom C6 of the polyunsaturated chain, while the HFE

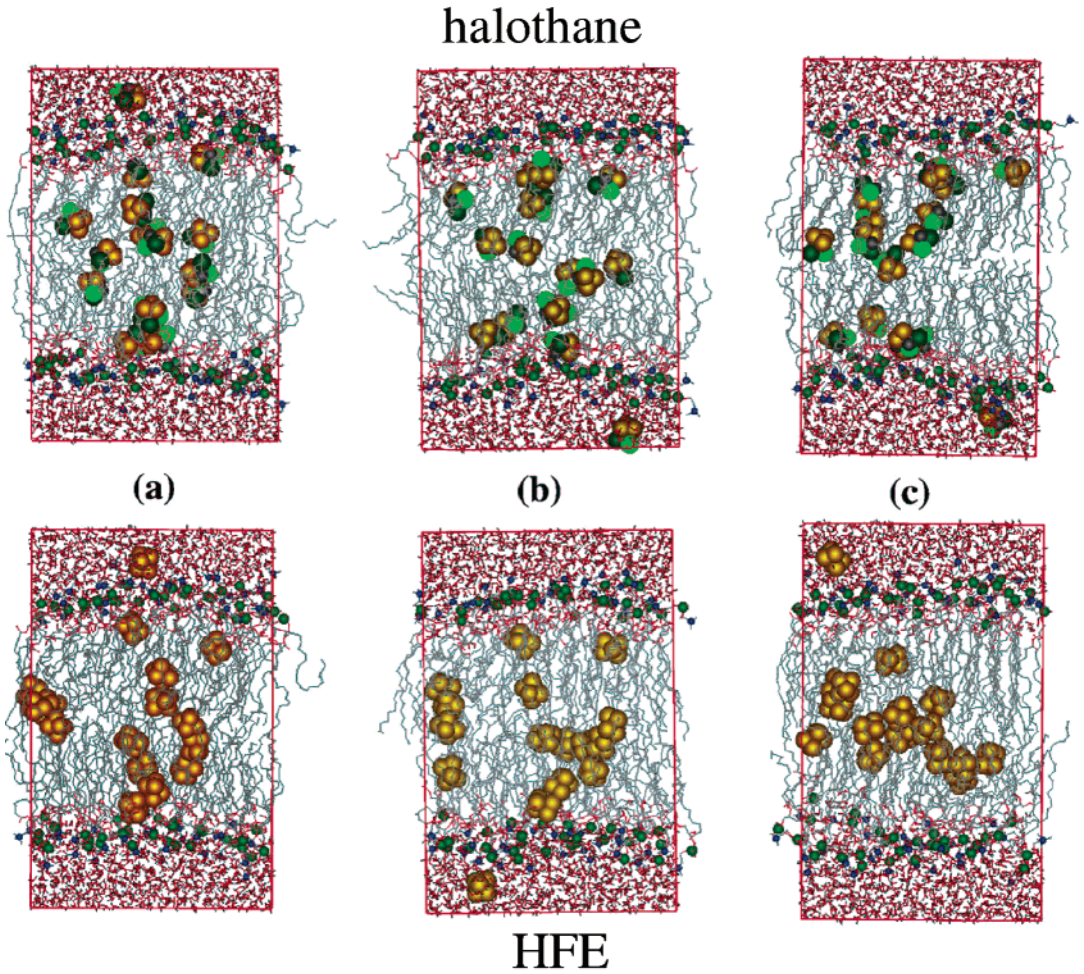

Figure 3. Instantaneous views (*XZ*) of configurations taken from the simulations of the SDPC/halothane system (top) and the SDPC/hexafluoroethane (HFE) system (bottom) with a lipid/solute ratio of 4/1. The three panels (a), (b), and (c) depict the systems at the end of the constant volume (NVT) equilibration runs (200 ps) and at 2 ns and 3.7 ns of the constant pressure (NPT) runs, respectively. Halothane and HFE are rendered with atomic van der Waals radii (F, orange; Cl, green; Br, dark green; H, gray). The lipid P and N atoms are displayed with covalent radii in green and blue, respectively. The water molecules (red) are represented using sticks. The lipid hydrogen atoms are omitted for clarity. Note the distinct distribution of the solutes within the lipid core. In both simulations, one molecule has migrated to the aqueous phase. When the diffusing solute leaves the simulation box, the periodic boundary condition cause it to enter from the opposite side of the box.

distributions are measurable only below the carbon atoms C11 and C15 of the saturated and polyunsaturated chains, respectively.

The accessibility of the lipid−water interface by the solute molecules can be inferred from the overlapping density distribution profiles of water and halothane/HFE molecules. The data presented in Figure 4 indicate that halothane molecules are more likely than HFE molecules to have access to the complex interface, where water molecules and lipid headgroups interact with each other and possibly with the solute molecules. The partial radial distribution functions, $g_{\alpha\beta}(r)$, are ordinarily calculated to study the structure of liquids and are very useful to evaluate whether the halothane and/or HFE molecules interact with water or the overlapping distributions are due to the fluctuations of the model membrane. Therefore, of particular interest to study solute hydration are those involving solute and water molecules. Concretely, we calculated the radial distribution functions $g_{O_wF}(r)$ of the oxygen atom of water around the fluorine atom of the individual halothane molecules in the SDPC/halothane system and compared the results in Figure 5 with those of a aqueous solution at similar conditions (from ref 32). Our analysis indicates that about half of the 16 halothane molecules (thin lines in Figure 5) have a $g_{O_wF}(r)$ similar to that of halothane in aqueous solution (bold dashed line in Figure 5), i.e., the first peak of the g(r) and the first minimum are located at similar positions. The rest of the molecules do not have access to water, and their $g(r)$ functions are null up to distances above 6 Å. As expected, the $g(r)$ functions are dependent on the solute location, and for those molecules located away from the lipid−water interface, the $g_{O_wF}(r)$ function lacks the structured features of halothane in aqueous solution. This is consistent with ^{19}F NMR chemical-shift analysis of anesthetic compounds in membranes,[24,26] where it was concluded that the anesthetics distribute preferentially in regions of the membrane that allow easy contact with water. A similar analysis for the HFE molecules (data not shown) indicates that practically none of the solute molecules is interacting with water, even though there is some overlapping between water and HFE density distributions (Figure 4).

The affinity of the anesthetic molecules to the upper part of the lipid acyl chains was previously observed for saturated lipids at higher concentrations (50% mole fraction of halothane in DPPC) and temperature ($T = 50$ °C) and using slightly different parameters for the force field (mainly for the atoms of the lipid headgroup).[33] The finding that the halothane molecules have a tendency to populate these regions at the expense of the rest of the lipid hydrophobic core agrees well with free energy profile estimates on model membranes with saturated lipids.[29,30] For

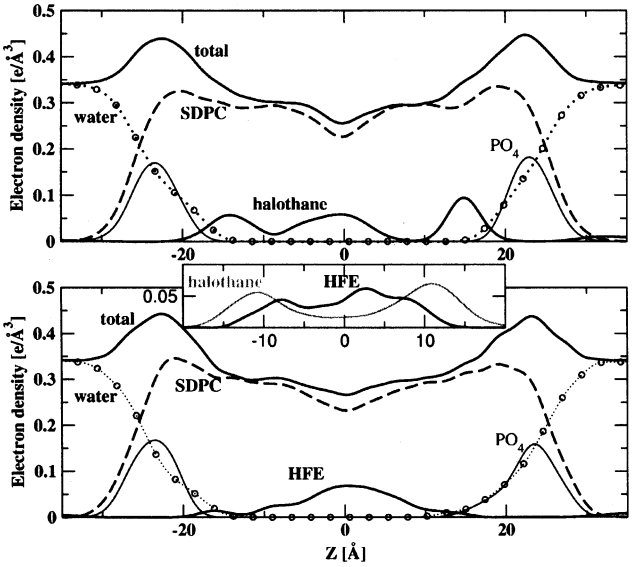

Figure 4. Electron-density distributions of halothane (top) and HFE (bottom) molecules within the SDPC lipid bilayer. We show the electron density profiles of the solutes, the lipid, and the water molecules along the bilayer normal (Z). $Z = 0$ Å corresponds to the bilayer center (methyl trough). In addition, the distribution of the phosphate groups (PO_4) of the lipids has been included to indicate the position of the lipid headgroups and, thus, of the lipid−water interface. Halothane and HFE density profiles have been conveniently augmented for clarity. It is worth noting that the HFE distribution is centered at $Z = 0$ Å and agrees well with earlier studies of HFE in a DMPC lipid bilayer. Moreover, the halothane distribution is bimodal, as observed in previous studies of halothane in a DPPC lipid bilayer. In addition, the halothane distribution presents another maximum around $Z = 0$ Å, which is missing in previous studies, and is associated with the presence of the highly unsaturated chains of the SDPC lipid. For the sake of clarity, we plot in the inset the electron-density profiles corresponding to 32 halothane molecules and 16 HFE molecules in a DPPC lipid bilayer (from ref 33) and in a DMPC lipid bilayer (from ref 35), respectively.

the nonanesthetic HFE molecules, previous studies on saturated (DMPC) lipid bilayers at similar (25% mole fraction) and lower (6% mole fraction) concentrations[34,35] indicated no affinity of the solute molecules to the upper part of the lipid molecules and a tendency to be located near the methyl trough. Consistently, the overall distributions observed in this study are similar to the previous simulations of saturated lipid bilayers (see Figure 4, inset).

Interestingly, in the case of the polyunsaturated SDPC lipid bilayer, however, we observed an additional maximum of the anesthetic concentration in the middle of the lipid bilayer even though the solute−lipid mole fraction is lower than the 50% used for the saturated DPPC lipid. This feature can be understood in terms of the unique properties of the SDPC pure lipid bilayers.[43,46,47] Indeed, the polyunsaturated chains of the SDPC molecules have the tendency to visit the lipid−water interface, and thus, the density profiles of the DHA chains have a maximum close to each of the lipid−water interfaces, missing for the stearoyl chains and other model membranes with saturated lipids.[43] This feature suggests that there would be more volume available at the center of the lipid bilayer than in disaturated lipid bilayers to be occupied by the halothane molecules. Consistently, the volume of the SDPC/halothane system increased from 137.5 ± 1.0 nm^3 to 139.2 ± 1.4 nm^3 after adding 16 halothane molecules, while the volume of the DPPC/halothane system increased from 134.1 ± 0.8 nm^3 to 141.0 ± 1.2 nm^3 after adding 32 halothane molecules. Assuming that the partial volume of the halothane molecule in solution is approximately 106 cm^3/mol (the mean partial molar volume of

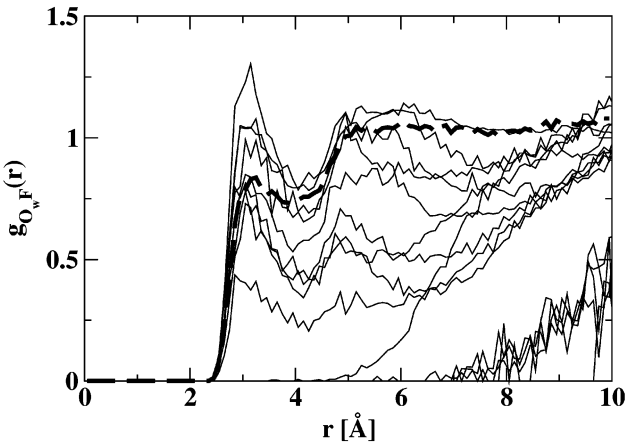

Figure 5. Radial pair distribution functions $g_{O_wF}(r)$ of the oxygen atoms of the water molecules around the fluorine atoms of the 16 individual halothane molecules embedded in the SDPC lipid bilayer (thin solid lines) and the corresponding $g_{O_wF}(r)$ of water molecules around halothane in a dilute aqueous solution (bold dashed line; from ref 32). Note that the $g(r)$ of about half of the halothane molecules is similar to that of halothane in an aqueous solution.

halothane in a DMPC lipid bilayer at 25 °C calculated from the excess volumes measured experimentally),[64] the volumes occupied by 16 and 32 molecules are 2.8 nm^3 and 5.6 nm^3, respectively. In both cases, the volume expansion is basically accounted for by the presence of solute and no additional free volume is created in agreement with experiment.[1,2] For the SDPC/halothane system, however, the volume expansion is slightly smaller than the volume occupied by the added solute. In addition to excluded volume effects, there can also be at play electrostatic interactions coming from the C=C groups (double bonds) of the polyunsaturated chains, which are more polar than the methylene groups, and the amphiphilic anesthetic molecules at the membrane trough. Simulation studies are currently under way to evaluate the importance and role of specific interactions between unsaturated lipid chains and anesthetic compounds.[65]

Although halothane and HFE distributions within the lipid bilayer are different, their effects on the overall membrane structure at the studied concentration appear to be similar, as reported in the previous section. The modest interlamellar spacing increase of about 7% is similar to the 8% observed in the HFE/DMPC system at similar conditions. The trend observed for halothane in DPPC lipid bilayers from previous simulations at higher concentrations, where halothane molecules induced an increase of the area per lipid molecule and a decrease of the lamellar spacing,[33] differs, however, from that observed here for the highly unsaturated SDPC lipid. The increase of the lamellar spacing for both anesthetic and nonimmobilizer molecules seems to be mainly due to the molecules located near the bilayer center. This additional anesthetic distribution was not observed in the case of the halothane/DPPC system, and thus, the addition of the solute caused an increase of the area per lipid and a decrease of the distance between the lamellae, which is partially caused by the redistribution of the water molecules within the simulation cell.[66] These discrepancies could be in part due to the different temperatures and concentrations studied for the different lipid bilayers and their different characteristics, such as the main phase-transition temperatures. The halothane/DPPC system was studied at higher concentrations (50% mole fraction) and temperature ($T = 50$ °C), which is 9 °C higher than the main transition temperature of the lipid ($T_m = 41$ °C), and using slightly different parameters for the force field.[33] The HFE/DMPC system was studied at a similar

concentration (25% mole fraction) and temperature ($T = 30$ °C), which is 7 °C higher than the main transition temperature of the lipid ($T_m = 23$ °C). The temperature studied for the SDPC lipid bilayer in all cases is $T = 30$ °C, which is 36 °C above the main transition temperature ($T_m = -6.5$ °C).

C. Acyl Chain Orientational Order Parameters. The behavior of acyl chains in lipid bilayers is usually studied through the orientational order parameters, S_{CD}. The S_{CD} can be obtained experimentally by NMR spectroscopy from the directly measured quadrupolar splitting, $\Delta\nu_Q$, using the relationship $\Delta\nu_Q = {}^3/_4(e^2qQ/h)S_{CD}$, where e^2qQ/h is the quadrupolar coupling constant. By site-directed deuteration of the different hydrogen atoms in the acyl chains, the experimental order parameter profile, $S_{CD}(n)$, can be derived for each position, n, along the deuterated chain. In the MD simulations, the orientational order parameter profile can be obtained directly and is given by[61] $S_{CD}(n) = {}^1/_2\langle 3\cos^2\beta_n - 1\rangle$, where β_n is the angle between the orientation of the vector along a C−H bond of the nth carbon atom of the saturated (sn1) and/or the polyunsaturated (sn2) chains and the bilayer normal. Here, the brackets indicate averages over time and lipid molecules. Since S_{CD} takes a value of 1 when the reference vectors are parallel, a value of −0.5 when the reference vectors are perpendicular, and a value close to zero for random orientations, the $-S_{CD}(n)$ values for lipid bilayers are usually in the range of 0−0.5.

Previous MD studies have shown that there is a strong effect of cis double bonds on the orientational order of the unsaturated chains (see, for instance, refs 43 and 58). Experimental studies[42,62,63] and MD simulations[44] have indicated that the polyunsaturated chains affect the order of the saturated chains. As a general trend, the different molecular structure and dynamics of the polyunsaturated chain lead to values of the order parameters significantly lower than those of the saturated chain.[43,46]

In Figure 6, we display the order parameter profile $-S_{CD}(n)$ for the carbon atoms along the saturated and polyunsaturated chains. The results obtained in the presence of the halothane and HFE molecules are compared to those obtained from the neat SDPC lipid bilayer.[43] The addition of anesthetic and nonimmobilizer solutes appears to have almost no effect on the lipid order parameters for the polyunsaturated chain, and thus, the $-S_{CD}(n)$ are close to zero for most of the positions.

In the case of HFE, we observed a modest increase of order parameters of the saturated chain for those carbon atoms located at the lower half of the chains. The halothane molecules, however, seem to have less effect on the saturated acyl chain order parameters, which are similar to those of the pure SDPC lipid bilayer, than found in previous theoretical[32,33] and experimental[25,26] investigations using saturated lipids or lipids with a low degree of unsaturation. For the high concentration DPPC/halothane system,[33] it was found that the presence of halothane molecules in the upper part of the acyl chain region induced a decrease in the order parameters for the terminal carbon atoms. The increase of the surface area per lipid molecule produced enough free volume around the DPPC lipid chain tails to allow for more flexibility and, thus, lower $-S_{CD}$ values. In polyunsaturated lipids, however, the presence of the HFE molecules at the bilayer center and the decrease observed in the area per lipid molecule induces a rearrangement of the more flexible and disordered polyunsaturated chains close to the lipid−water interface. An increase of the population of linear conformations of the DHA chain in this region would result in a modification of the order parameters of the saturated chains in their bottom half. This is consistent with previous observations that linear

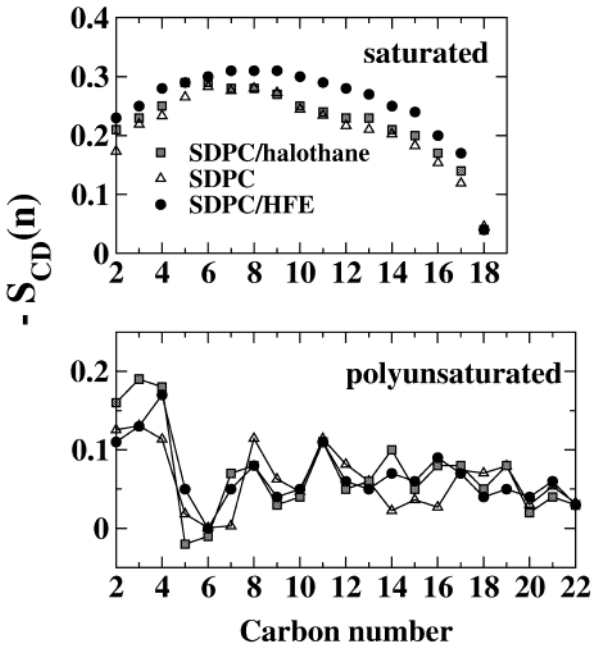

Figure 6. Deuterium orientational order parameters ($-S_{CD}$) as a function of the position of the carbon atoms along the hydrocarbon chains of the SDPC lipid molecules for the saturated (top) and the polyunsaturated (bottom) chains. The different curves correspond to the results obtained for the SDPC/halothane (grey squares) and SDPC/HFE (black circles) systems and are compared to those of a pure SDPC lipid bilayer (triangles) from ref 43.

conformations of regions of the DHA chains close to the lipid headgroup increase the order of the bottom half of the saturated chains, while nonlinear conformations decrease the order.[44] In the case of the anesthetic molecules, the effect of the halothane distribution at the membrane center is compensated by the bimodal halothane distribution at the lipid−water interface. While the former will increase the $-S_{CD}$ values at the bottom half of the chains as occurs for the HFE molecules, the latter will increase the disorder in the same region.

The effect of the solutes on the internal dynamics of the lipids can be studied by monitoring the reorientational relaxation of the SDPC acyl chains. Here, the reorientational molecular motions have been analyzed through the time correlation functions $C(t) = \langle(3\cos^2(\theta(t)) - 1)/2\rangle$, where $\theta(t)$ is the angle through which the considered molecule-fixed vector rotates in a time t. We calculated $C(t)$ for the vector along the C_n−H bond for $n = 2, ..., 18$ of the saturated chain. These reorientational correlation functions generally consist of a fast (100 ps) and a slow (1 ns) component.[67] Our results for the halothane and HFE solutes (data not shown) and those of the pure SDPC lipid bilayer[48] indicate that the presence of the solutes (both anesthetic and nonimmobilizer molecules) has essentially no effect on the reorientational motions, and thus, the fluidity of the membrane with highly unsaturated lipids seems to be preserved at this concentration (25%). Investigation of the mean-squared displacements of centers of mass of the lipid molecules, both in-plane and out-of-plane (data not shown), reveal a slight slowing down of both motions as HFE or halothane molecules are added to the pure lipid bilayer.

D. Lipid−Water Interface. In our earlier simulations, we observed that the distribution of halothane molecules in the upper part of the lipids (close to the lipid−water interface) caused a global reorientation of the lipid phosphatidylcholine headgroup dipole moments, while this effect was not observed in the presence of the nonimmobilizer HFE. To quantitatively

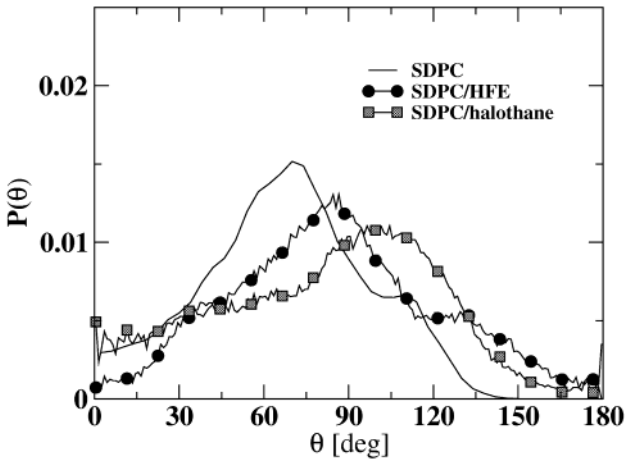

Figure 7. Orientational probability distribution $P(\theta)$ of the θ angle between the headgroup P−N vector (essentially the headgroup dipole moment) and the bilayer normal in arbitrary units. The results for the SDPC/halothane (■) and SDPC/HFE (●) systems are compared with those for the pure lipid bilayer from ref 45 (−). Note that the presence of either solute slightly shifts the average orientation of the lipid headgroups (from about 70° for pure SDPC to about 85° for the mixed systems) and causes the headgroups to point more toward the membrane surface. In addition, only in the case of halothane, the most probable orientation is now greater than 90° (105°); i.e., most of the P−N vectors point toward the membrane interior.

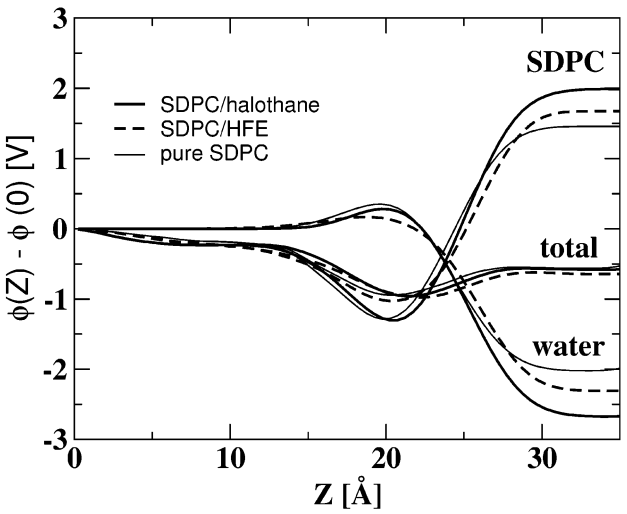

Figure 8. Electrostatic potential profile relative to that at the bilayer center, $Z = 0$ Å, i.e., $\phi(Z) - \phi(0)$, for the SDPC/halothane system (solid bold lines) and the SDPC/HFE system (dashed bold lines). The results are compared with those obtained for the pure SDPC lipid bilayer in ref 45 (solid thin lines). The individual contributions arising from the water and the lipid molecules are plotted separately.

evaluate the effect of the solutes for the SDPC lipid bilayer, we investigated the orientation of the headgroup dipole moment (basically, the P → N vector, denoted by P−N) of the lipid with respect to the membrane normal. In Figure 7, we display the probability distribution of angles θ, namely, $P(\theta)$, between the lipid headgroup P−N vectors and the bilayer normal, $\hat{n}$, for the halothane/SDPC, HFE/SDPC, and the pure SDPC lipid bilayer[45] systems. For the polyunsaturated lipid, the changes observed for the headgroup P−N dipole orientation due to the presence of the two types of solute are consistent with previous observations for the saturated lipids.

The most probable values for the θ angles of the three different systems shown in Figure 7 are 70° (pure SDPC lipid bilayer),[45] 85° (SDPC/HFE), and 105° (SDPC/halothane). These results agree well with the general trend observed in saturated lipids, i.e., 75° (HFE) and 120° (halothane).[33,35] Note that $\theta = 0°$, $\theta = 90°$, and $\theta = 180°$ correspond to the direction of the bilayer normal ($\hat{n}$), the membrane surface, and the direction opposite to the bilayer normal ($-\hat{n}$), respectively. We have also calculated the average values for the θ angles, which are 69° (pure SDPC lipid bilayer),[45] 85° (SDPC/HFE), and 82° (SDPC/halothane). It is interesting to note that the addition of the solutes causes the average value of the angle between the lipid headgroup dipoles to increase about 15°. On average, the P−N vectors point less toward the water region and, thus, lie more at the lipid−water interface independently of the type of solute probably due to the small decrease in the area per lipid molecule upon addition of the solutes. In contrast, the halothane and HFE molecules affect differently how most of the lipid headgroups behave in the mixed systems, i.e., the most probable orientation of the dipole moments. Compared to the pure SDPC lipid bilayer, the HFE molecules slightly shift the main maximum of $P(\theta)$ toward higher angles (and also the smallest maximum at $\theta = 110°$) and lower the probability of finding lipid headgroups aligned with the bilayer normal. The halothane molecules, in contrast, change quantitatively the picture observed for the pure lipid bilayer by increasing the probability for a lipid headgroup dipole to be pointing toward the lipid hydrocarbon region, while there are still P−N vectors with orientations in the 0−70° range. The small maximum at about $\theta = 110°$ observed for the pure lipid bilayer now becomes the most probable orientation for the dipole moments. The results obtained for the halothane/HFE influence on the lipid headgroup dipole orientations are in excellent agreement with previous observations in saturated lipid bilayers[33−35] and, thus, confirm the different effects of anesthetics and nonimmobilizers on the electrostatic properties of the lipid−water interface, which may be linked to their different clinical effects and therefore might contribute to the mechanism of general anesthesia.

The differences observed in the orientational probability distributions of the lipid headgroup dipoles with respect to the bilayer normal may affect the charge distribution in the direction of the membrane normal and, consequently, the electrostatic potential across the interface (membrane potential). The electrostatic potential profile, $\phi(Z)$, can be estimated using Poisson's equation, which reads $-\nabla^2\phi(Z) = (1/\epsilon_0)\rho(Z)$, with $\rho(Z)$ being the charge density as a function of Z. Thereby, the electrostatic potential across the membrane is given by $\phi(Z) - \phi(0) = -1/\epsilon_0 \int_0^Z \int_0^{Z'} \rho(Z'')\, dZ''\, dZ'$, where $\phi(0)$ is the electrostatic potential at the bilayer center. In Figure 8, the potential difference $\phi(Z) - \phi(0)$ is plotted as a function of Z for the two mixed systems and the pure SDPC lipid bilayer. To investigate the origin of the different features of the curves, we calculated the contributions due to the lipid and the water molecules, which are plotted separately in Figure 8. The components arising from the water and lipid molecules display a trend going from the pure lipid to the HFE/SDPC and finally to the halothane/SDPC systems, where the absolute value of the corresponding contribution to the membrane potential increases (SDPC < SDPC/HFE < SDPC/halothane). The results obtained for the membrane potential of the SDPC/halothane (−570 mV) and SDPC/HFE (−650 mV) systems are very similar to those computed for the pure lipid (−550 mV).[45,68]

IV. Conclusion

We have investigated the effect of anesthetics and their nonimmobilizer analogues on the physical properties of simple model membranes containing lipids with highly unsaturated acyl

chains at conditions relevant to biology. Specifically, we have carried out two MD simulations of a fully hydrated SDPC lipid bilayer in the liquid crystalline phase L_α with a 25% mole fraction of the anesthetic halothane and the nonanesthetic hexafluoroethane. The results obtained have been compared with previous simulations of the same solutes in saturated lipid bilayers[32−35] and with previous studies of the pure SDPC lipid bilayer system.[43−45,48]

Our results indicate that anesthetic and nonanesthetic molecules exhibit different distributions along the direction parallel to the membrane normal and are similar to those observed in other studies on saturated lipid bilayers.[32−35] In agreement with our previous simulations, the halothane molecules display a nonuniform (bimodal) distribution, indicating an increase in the number of anesthetic molecules near the upper part of the lipid acyl chains, i.e., close to the lipid headgroups and membrane interface, while HFE molecules are located mostly at the bilayer center (methyl trough) and acyl chain region. In addition, the halothane distribution for the polyunsaturated system presents another maximum at the methyl trough. This seems to be caused by the tendency of the polyunsaturated chains to visit the lipid−water interface. Additionally, since C═C groups (double bonds) are more polar than methylene groups,[43] the amphiphilic anesthetic molecules may participate in electrostatic interactions with the polyunsaturated chains at the membrane center. Simulation studies are currently under way to evaluate the importance and role of specific interactions between unsaturated lipid chains and anesthetics.[65] The present study is important for the further understanding of simple systems consisting of a four-α-helix bundle scaffold with a hydrophobic core[69,70] as simple models for studying the structural features of volatile anesthetic binding sites on proteins because it provides insights into the behavior of halothane molecules in different types of *hydrophobic* environments. The calculation of the radial distribution functions of water molecules around the halothane molecules indicates that half of the anesthetic molecules present an environment similar to that of halothane in aqueous solution. Even though the present results have been obtained for concentrations of solutes quite high compared to those typical of clinical use, it is reasonable to expect that the different distributions for anesthetic and nonanesthetic molecules within the membrane will be similar at lower concentrations.

At the studied concentration, the presence of both solutes caused subtle structural changes of the membrane system. Specifically, we observed an increase of the lamellar spacing and a decrease of the area per lipid for halothane and HFE. This trend is similar to that found previously in DMPC/HFE systems but opposite to previous results at higher concentrations in DPPC/halothane systems. Similar discrepancies are observed for the effects of the solutes on the different properties of the membrane interior, such as the orientational order parameters of the hydrocarbon chains and dynamical properties, when polyunsaturated and saturated lipids are compared due to the unique properties of polyunsaturated chains. For the HFE molecules, we observed a modest increase of the orientational order parameters of the hydrocarbon chains for those carbon atoms located at the lower half of the saturated chains. The tendency for the halothane molecules to be located close to the interface seems to compensate this effect, and the order parameters are similar to those of the pure SDPC lipid bilayer. The dynamical properties studied, i.e., the reorientational motions of the saturated acyl chains and the mean-squared displacement of the molecular centers of mass, are essentially not affected by the solutes. Even though we did not observe clear different trends for anesthetics and nonanesthetics systems on the properties of the membrane interior, our results do not rule out that these small differences might create important changes in the lateral pressure profiles, for instance, as suggested by Cantor.[9−11]

The organization of the lipid headgroup dipole moments at the lipid−water interface is modified differently by the two solute types. The addition of the solutes causes the average value of the angle between the headgroup dipole and the membrane normal to slightly increase. On average, headgroup dipoles point less toward the water region independently of the solute type. In contrast, halothane and HFE molecules affect differently the most probable orientation of the dipoles. For HFE, the most probable orientation is slightly shifted toward an angle closer to the membrane surface but similar to that of the pure system. In the case of halothane, most of the dipoles are now pointing toward the lipid hydrocarbon chains. This important difference between anesthetics and nonimmobilizers is consistent with our previous observations in saturated lipid bilayers.

In summary, our results indicate that the different distributions of anesthetic and nonimmobilizer molecules within the lipid bilayer systems seem to be a generic feature in simple models of biological membranes. Since polyunsaturated and other unsaturated lipids are ubiquitous in cell membranes, it is plausible to generalize these features to the more complex biological membranes.

Acknowledgment. This work has been supported by the National Institutes of Health through Grant No. P01 GM 55876. Computer facilities were provided by the National Center for Supercomputing Applications. L.S. gratefully acknowledges support from the NIST Center for neutron research of the National Institute of Standards and Technology (Grant Ref. No. 5H0014). We thank Prof. R. G. Eckenhoff for useful comments on an early version of the manuscript.

References and Notes

(1) Franks, N. P.; Lieb, W. R. *Nature* **1994**, *367*, 607.
(2) Trudell, J. R.; Hubell, W.; Cohen, E. N. *Biochim. Biophys. Acta* **1973**, *291*, 321.
(3) Pringle, M. J.; Miller, K. W. *Biochemistry* **1979**, *18*, 3314.
(4) Koehler, L. S.; Fossel, E. T.; Koeler, K. A. In *Molecular mechanism of anesthesia*; Fink, E., Ed.; Raven Press: New York, 1980; p 447.
(5) Miller, K. W. *Int. Rev. Neurobiol.* **1985**, *27*, 1.
(6) Curatola, C.; Lenaz, G.; Zolese; G. In *Drugs and Anesthetic Effects on Membrane Structure and Function*; Abia, L. C., Curtain, C. C., Gordon, L. M., Eds.; Wiley-Liss: New York, 1991; p 35.
(7) Mihic, S. J.; Ye, Q.; Wick, M. J.; Koltchine, V. V.; Krasowski, M. D.; Finn, S. E.; Mascia, M. P.; Valenzula, C. F.; Hanson, K. K.; Greenblatt, E. P.; Harris, R. A.; Harrisson, N. L. *Nature* **1997**, *389*, 385.
(8) Eckenhoff, R. G.; Johanson, J. S. *Pharmacol. Rev.* **1997**, *49*, 343.
(9) Cantor, R. S. *Biochemistry* **1997**, *36*, 2339.
(10) Cantor, R. S. *J. Phys. Chem. B* **1997**, *101*, 1723.
(11) Cantor, R. S. *Biophys. J.* **1999**, *76*, 2625.
(12) Meyer, K. H. *Trans. Faraday. Soc.* **1937**, *33*, 1062.
(13) Miller, K. W.; Smith, E. B. In *A guide to Molecular Pharmacology-Toxicology*; Featherstone; R. M., Ed.; Decker: New York, 1973; Vol.1, p 427.
(14) Koblin, D.; Chortkoff, B.; Laster, M.; Eger, E.; Halsey, M.; Ionescu, P. *Anesthesiology* **1994**, *79*, 1043.
(15) Kandel, L.; Chortkoff, B. S.; Sonner, J.; Laster, M. J.; Eger, E. *Anesth. Analg.* **1996**, *82*, 321.
(16) Fang, Z.; Laster, M. J.; Ionescu, P.; Koblin, D.; Sonner, J., Eger, E.; Halsey, M. J. *Anesth. Analg.* **1997**, *85*, 1149.
(17) Minima, K.; Vanderah, T. W.; Minima, M.; Harris, R. A. *Eur. J. Pharm.* **1997**, *339*, 237.
(18) Raines, D. E. *Anesthesiology* **1996**, *84*, 663.
(19) Forman, S. A.; Raines, D. E. *Anesthesiology* **1998**, *88*, 1535.
(20) Xu, Y.; Tang, P.; Liachenko, S. *Toxicology Lett.* **1998**, *101*, 347.
(21) Lieb, W. R.; Kovalycsik, M.; Mendelsohn, R. *Biochim. Biophys. Acta* **1982**, *688*, 388.

(22) Craig, N. C.; Bryant, G. J.; Levin, I. W. *Biochemistry* **1987**, *26*, 2449.
(23) Tsai, Y. S.; Ma, S. M.; Kamaya, H.; Ueda, I. *Mol. Pharmacol.* **1987**, *26*, 603.
(24) Tang, P.; Yan, B.; Xu, Y. *Biophys. J.* **1997**, *72*, 1676.
(25) Baber, J.; Ellena, J. F.; Cafiso, D. S. *Biochemistry* **1995**, *34*, 6533.
(26) North, C.; Cafiso; D. S. *Biophys. J.* **1997**, *72*, 1754.
(27) Saiz, L.; Klein, M. L. *Acc. Chem. Res.* **2002**, *35*, 482.
(28) Pastor, R. W., Venable, R. M.; Feller, S. E. *Acc. Chem. Res.* **2002**, *35*, 438.
(29) Pohorille, A.; Cieplak, P.; Wilson, M. A. *Chem. Phys.* **1996**, *204*, 337.
(30) Pohorille, A.; Wilson, M. A. *J. Chem. Phys.* **1996**, *104*, 3760.
(31) Pohorille, A.; Wilson, M. A.; New, M. H.; Chipot, C. *Toxicology Lett.* **1998**, *101*, 421.
(32) Tu, K.; Tarek, M.; Klein, M. L.; Scharf, D. *Biophys. J.* **1998**, *75*, 2123.
(33) Koubi, L.; Tarek, M.; Klein, M. L., Scharf, D. *Biophys. J.* **2000**, *78*, 800.
(34) Koubi, L.; Tarek, M.; Bandyopadhyay, S.; Klein, M. L.; Scharf, D. *Biophys. J.* **2001**, *81*, 3339.
(35) Koubi, L.; Tarek, M.; Bandyopadhyay, S.; Klein, M. L.; Scharf, D. *Anesthesiology* **2002**, *97*, 848.
(36) Salem, N., Jr. In *New protective Roles for selected Nutrients*; Spiller, G. A., Scala, J., Eds.; Alan R. Liss: New York, 1989; p 109.
(37) Huster, D.; Jin, A. J.; Arnold, K.; Gawrisch, K. *Biophys. J.* **1997**, *73*, 855.
(38) Olbrich, K.; Rawicz, W.; Needham, D.; Evans, E. *Biophys. J.* **2000**, *79*, 321.
(39) Koenig, B. W.; Strey, H. H.; Gawrisch, K. *Biophys. J.* **1997**, *73*, 1954.
(40) Rawicz, W.; Olbrich, K. C.; McIntosh, T.; Needham, D.; Evans, E. *Biophys. J.* **2000**, *79*, 328.
(41) Barry, J. A.; Trouard, T. P.; Salmon, A.; Brown, M. F. *Biochemistry* **1991**, *30*, 8386.
(42) Salmon, A.; Dodd, S. W.; Williams, G. D.; Beach, J. M.; Brown, M. F. *J. Am. Chem. Soc.* **1987**, *109*, 2600.
(43) Saiz, L.; Klein, M. L. *Biophys. J.* **2001**, *81*, 204.
(44) Saiz, L.; Klein, M. L. *J. Am. Chem. Soc.* **2001**, *123*, 7381.
(45) Saiz, L.; Klein, M. L. *J. Chem. Phys.* **2002**, *116*, 3052.
(46) Feller, S. E.; Mackerell, A. D., Jr.; Gawrisch, K. *J. Am. Chem. Soc.* **2002**, *124*, 318.
(47) Huber, T.; Rajamoorthi, K.; Kurze, V. F.; Beyer, K.; Brown, M. F. *J. Am. Chem. Soc.* **2002**, *124*, 298.
(48) Saiz, L.; Klein, M. L., to be published.
(49) Pang, K.-Y. Y.; Braswell, L. M.; Chang, L.; Sommer, T. J.; Miller, K. W. *Mol. Pharmacol.* **1980**, *18*, 84.
(50) Tuckerman, M. E.; Yarne, D. A.; Samuelson, S. O.; Hughes, A. L.; Martyna, G. J. *Comput. Phys. Comm.* **2000**, *128*, 333.
(51) Martyna, G. J.; Tuckerman, M. E.; Tobias, D. J.; Klein, M. L. *Mol. Phys.* **1996**, *87*, 1117.
(52) Darden, T.; York, D.; Pedersen, L. *J. Chem. Phys.* **1993**, *98*, 10089.
(53) Essmann, U.; Perera, L.; Berkowitz, M. L.; Darden, T.; Pedersen, L. G. *J. Chem. Phys.* **1995**, *103*, 8577.
(54) Allen, M. P.; Tildesley, D. J. *Computer Simulation of liquids*; Clarendon: Oxford, 1987.
(55) Schlenkrich, M.; Brickmann, J.; MacKerell, A. D., Jr.; Karplus, M. In *Biological membranes: A molecular perspective from computation and experiment*; Merz, K. M., Jr., Roux, B., Eds.; Birkhauser: Boston, 1996; p 31.
(56) Feller, S. E.; Mackerell, A. D., Jr. *J. Phys. Chem. B* **2000**, *104*, 7510.
(57) Jorgensen, W. L.; Chandrasekhar, J.; Madura, J. D.; Impey, R. W.; Klein, M. L. *J. Chem. Phys.* **1983**, *79*, 926.
(58) Feller, S. E.; Yin, D.; Pastor, R. W.; Mackerell, A. D., Jr. *Biophys. J.* **1997**, *73*, 2269.
(59) Hyvonen, M. T.; Rantala, T. T.; Ala-Korpela, M. *Biophys. J.* **1997**, *73*, 2907.
(60) Scharf, D.; Laasonen, K. *Chem. Phys. Lett.* **1996**, *258*, 276.
(61) Seelig, A.; Seelig, J. *Biochemistry*, **1974**, *13*, 4839.
(62) Rajamoorthi, K.; Brown, M. F. *Biochemistry* **1991**, *30*, 4204.
(63) Holte, L. L.; Peter, S. A.; Sinnwell, T. M.; Gawrisch, K. *Biophys. J.* **1995**, *68*, 2396.
(64) Kita, Y.; Bennet, L. J.; Miller, K. W. *Biochim. Biophys. Acta* **1981**, *647*, 130.
(65) Pickholz, M.; Saiz, L.; Klein, M. L., unpublished.
(66) Pickholz, M.; Klein, M. L., to be published.
(67) Venable, R. M.; Zhang, Y.; Hardy, B. J.; Pastor, R. W. *Science* **1993**, *262*, 223.
(68) To compare quantitatively the results presented here for the electrostatic potential along the membrane normal with those of refs 32−35, the data in refs 32−35 should be multiplied by a missing 4π factor for SI units.
(69) Johansson, J. S.; Scharf, D.; Davies, L. A.; Reddy, K. S.; Eckenhoff, R. G. *Biophys. J.* **2000**, *78*, 982.
(70) Davies, L. A.; Zhong, Q. F.; Klein, M. L.; Scharf, D. *FEBS Lett.* **2000**, *478*, 61.